ACS OMEGA

http://pubs.acs.org/journal/acsodf

Article

Microplasma-Enabled Surfaced-Functionalized Silicon Quantum Dots for Label-Free Detection of Dopamine

Gui-Yi Chang, Darwin Kurniawan, Yi-Ju Chang, and Wei-Hung Chiang*

Cite This: *ACS Omega* 2022, 7, 223−229

Read Online

ACCESS | Metrics & More | Article Recommendations | Supporting Information

ABSTRACT: Rapid and sensitive detection of dopamine (DA) is important for the diagnostics of neurological disorders and the development of new drugs. Here, we report microplasma synthesis of surfaced-functionalized silicon quantum dots (SiQDs) at ambient conditions. The synthesized SiQDs with useful properties including abundant surface functionalities, stable colloidal dispersion, and photoluminescence (PL) emission enable direct label-free detection of DA, providing a wide sensing range from 0.83 to 83.33 μM and a low detection limit of 0.32 μM. Our work provides a new direction for the synthesis of colloidal SiQDs and the understanding of SiQD-based PL probes for biomolecule sensing.

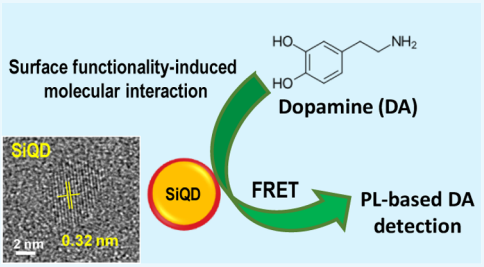

1. INTRODUCTION

Dopamine (DA) is an important neurotransmitter and plays a critical role in the central nervous systems of human bodies. The abnormal concentration of DA can lead to vital nervous system-related diseases including Parkinson's disease, schizophrenia, and depression.[1] The detections of DA are not only important for early detection and diagnostics of neurological disorders but also for the research and development of new drugs. While several technologies including high-performance liquid chromatography (HPLC)[2] and electrochemical analysis[3] have been developed to detect DA, they usually involve expensive and toxic materials, as well as complicated and time-consuming operations. Recently, optical spectroscopy-enhanced detection technologies such as surface-enhanced Raman scattering (SERS)[4−6] and photoluminescence (PL)-based[7−11] detections have been reported as emerging methods for DA sensing with high sensitivity. In particular, PL-based detection of DA using luminescent materials including metal nanoparticles, carbon and graphene nanoparticles, and silicon-based nanocrystals has drawn a lot of attention because of its advantages of not only high sensitivity but also good reliability, low cost, and simple operation.

Among the luminescent materials as PL probes for biosensing, recently, Si quantum dots (SiQDs) have been reported to have exceptional properties including tunable PL emissions, photostability against photobleaching, controllable surface functionalizations, and potential biocompatibility.[7−10] In addition, Si is an earth-abundant element with the advantages of chemical inertness, low cost, and nontoxicity and has been widely used in the semiconductor industry.[12,13] Moreover, the molecular interactions between analytes and Si surfaces can be enhanced via hydrogen bonds and/or electrostatic interaction through an appropriate surface functionalization of SiQDs, achieving label-free detection of DA with high sensitivity and selectivity.[7,14] However, the current SiQD synthesis methods including top-down approaches such as etching and electrochemical methods and bottom-up approaches such as hydrothermal and microwave methods are normally time-consuming and require expensive chemicals, high temperature, and complicated synthetic procedures.[15−20] Moreover, they usually involve toxic reducing agents, complicated stabilizers, and strong acids/bases during the synthesis. Overall, they still lack a simple and scalable method to synthesize surface-functionalized SiQDs with controlled structures for label-free detection of DA with high sensitivity and selectivity.

Here, we report a simple and scalable method to synthesize surface-functionalized SiQDs with controlled structures at ambient conditions using microplasmas and demonstrate that the plasma-synthesized SiQDs can be used for quantitative label-free detection of DA (Scheme 1a,b). Microplasmas represent the gaseous discharges with one dimension reduced to a micrometer-scale length.[21,22] By reducing the plasma size, the gas temperature is lower than the electron temperature, and the plasma can generate high density of reactive species including electrons, radicals, ions, and UV photons. Therefore, microplasmas classify a unique type of low-temperature, nonthermal equilibrium plasmas and have been shown to be a useful technology for material synthesis and processing, especially effective for nanomaterials including metal nanoparticles, carbon-based nanomaterials such as graphene and carbon quantum dots, and semiconductor-based nanomateri-

Received: August 17, 2021
Accepted: October 29, 2021
Published: November 26, 2021

Scheme 1. Schematic Illustration of Microplasma Synthesis of Surface-Functionalized SiQDs for Label-Free PL-Based Detection of DA[a]

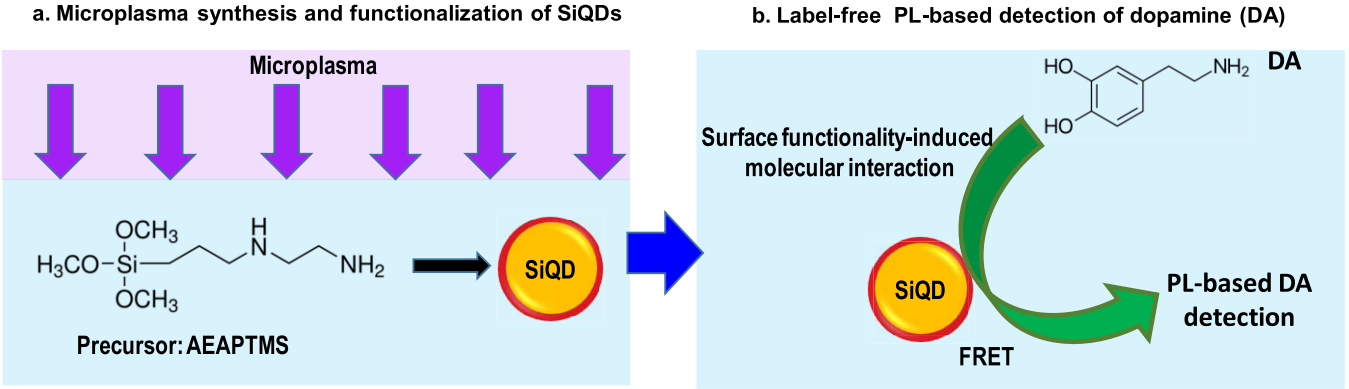

[a](a) One-step synthesis of SiQD nanosensors from [3-(2-aminoethylamino)propyl]trimethoxysilane (AEAPTMS) as a silicon precursor under ambient conditions using microplasmas. (b) Synergistic effect of surface functionality-induced molecular interaction and fluorescence resonance energy transfer (FRET)-induced PL quenching between SiQDs and DA for PL-based label-free detection of DA.

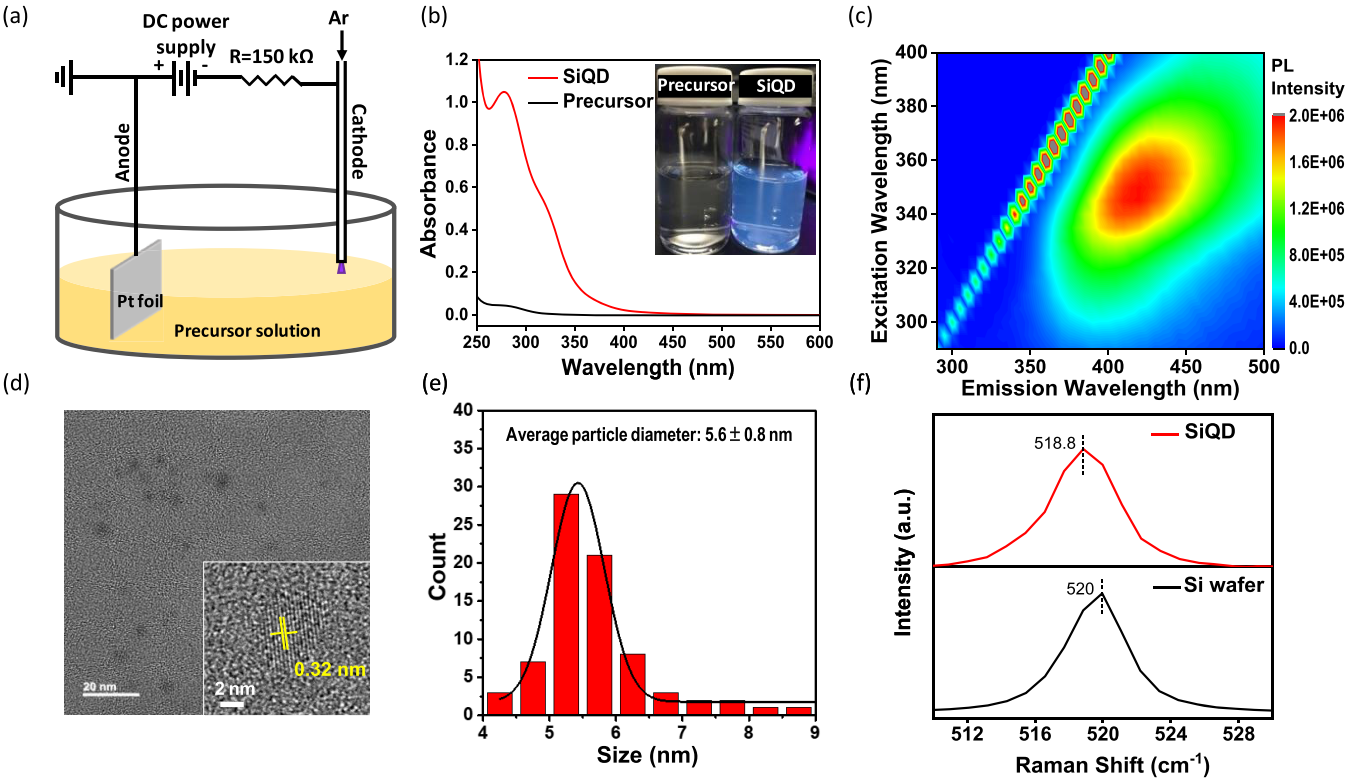

Figure 1. Synthesis and characterization of plasma-synthesized SiQDs. (a) Schematic illustration of the experimental setup for SiQD synthesis using microplasmas. (b) Ultraviolet−visible (UV−vis) absorbance spectra of plasma-synthesized SiQDs and the precursor. Inset: Photographs of SiQDs and the precursor under 365 nm UV-light irradiation. (c) PL map of plasma-synthesized SiQDs. (d) TEM image of SiQDs. Inset: HRTEM image with the lattice spacing of SiQDs. (e) Corresponding histogram of size distribution analyzed from TEM images. (f) Micro-Raman spectra of SiQDs and the Si wafer under 532 nm laser excitation.

als.[21,22] Moreover, the microplasmas with high densities of reactive species allow not only rapid synthesis of nanomaterials but also *in situ* surface functionalization of nanomaterials with controllable functionalities.[23,24] In this work, the colloidal SiQDs were synthesized and surface-functionalized from [3-(2-aminoethylamino)propyl]trimethoxysilane (AEAPTMS) as a silicon precursor at ambient conditions using microplasmas without adding toxic reducing agents and complicated stabilizers (Scheme 1a). AEAPTMS is a common aminosilane and is widely used for the surface functionalization of silica-based materials and in the semiconductor industry.[25] The plasma-synthesized SiQDs show stable colloidal dispersion with long-term stability up to 12 months and stable room-temperature blue photoluminescence emission at 420 nm. Moreover, the abundant surface functionalities on the SiQD surfaces can selectively attract the DA onto the SiQD surfaces without any complex surface modifications.[14] Previous reports have shown that surface functionalities play an integral part in the dispersibility and stability of SiQDs in a liquid medium, expanding the applicability of silicon-based nanomaterials in

https://doi.org/10.1021/acsomega.1c04467
ACS Omega 2022, 7, 223−229

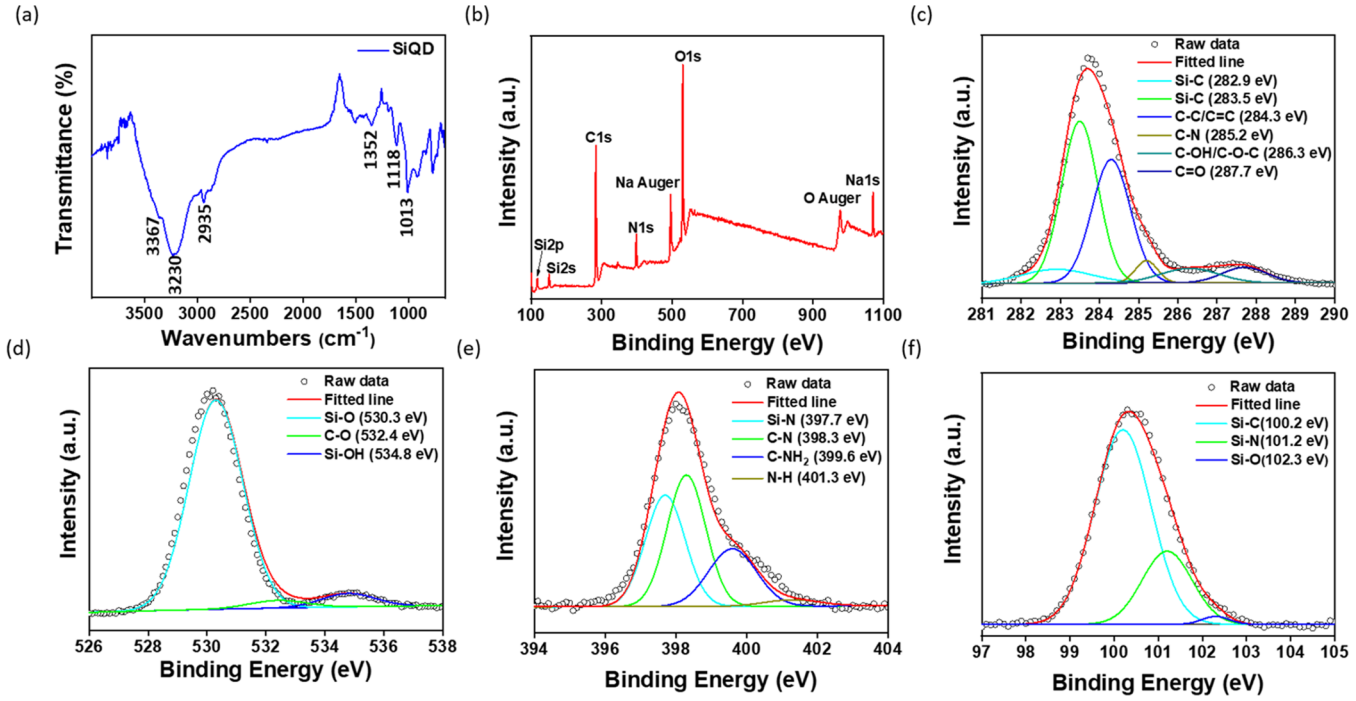

Figure 2. FTIR and XPS characterization of plasma-synthesized SiQDs. (a) FTIR spectrum of SiQDs. (b) Wide scan of the XPS spectrum of SiQDs. High-resolution XPS (c) C 1s, (d) O 1s, (e) N 1s, and (f) Si 2p spectra of SiQDs.

water-based applications.[26] In addition, higher PL quenching efficiency of SiQDs can also be expected upon the addition of DA owing to the possible generation of hydrogen bonding interaction between the surface functional groups of SiQDs with DA.[27] The synthesized SiQDs can directly be used as PL-based nanosensors for quantitative label-free detection of DA without any special treatment, providing a wide sensing range from 0.83 to 83.33 μM and a low detection limit of 0.32 μM (Scheme 1b). We propose the synergistic effect of surface functionality-induced molecular interaction via a hydrogen bond between DA and SiQDs and fluorescence resonance energy transfer (FRET)-induced PL quenching can be the factor to control the PL-based label-free detection of DA with SiQDs. Our work provides a step for scalable plasma synthesis of colloidal nanomaterials and understanding of the nanomaterial-enhanced PL-based chemical and biosensing.

2. RESULTS AND DISCUSSION

The SiQDs were synthesized in aqueous solutions using a direct current (dc) argon (Ar) microplasma electrochemical reactor operated at ambient conditions. The illustration of the experimental setup is schematically shown in Figure 1a, and details of the setup and synthesis can be found in the Supporting Information S1 and previous wok.[23] First, UV−vis spectroscopy was used to study the synthesis of SiQDs, and Figure 1b shows the absorbance spectra of the precursor and colloidal SiQDs prepared using microplasmas at 7 mA current and 30 min reaction time. It is shown that no absorbance band was noticed for the precursors before plasma treatment, while one peak with shoulders at 278 and 324 nm were respectively observed after the plasma reaction. These two absorbance features below 400 nm can be assigned to the n−π* electronic transitions of SiQDs, which is consistent with a previous report.[28] The inset shows the photographs of the SiQD dispersion in DI water exhibiting blue luminescence under 365 nm UV irradiation. PL spectroscopy was further used to probe the optical properties of the SiQDs, and the PL map indicates that SiQDs exhibit a maximum emission at 420 nm under 350 nm excitation at room temperature (Figure 1c). Transmission electron microscopy (TEM) was performed to study the morphology and crystallinity of SiQDs. The TEM image (Figure 1d) shows dispersed particle-like nanostructures almost free of an amorphous coating. The inset shows the high-resolution TEM (HRTEM) image of one individual SiQD with a 0.32 nm lattice fringe of the (111) plane of Si crystals (Figure 1d inset).[29,30] The corresponding histogram size distribution indicates an average size of 5.6 ± 0.8 nm by taking 30 different particles from the TEM images (Figure 1e). Raman spectroscopy is a useful method to identify the vibrational structures of Si-based nanomaterials.[31,32] Figure 1f displays the Raman spectra of a bulk Si wafer and the synthesized SiQDs. The bulk Si Raman peak at 520 cm^{-1} was observed while a shift to 518.8 cm^{-1} was noticed for the synthesized SiQDs. A previous report suggests that the bulk Si Raman peak can be down-shifted by decreasing the particle size of Si-based nanomaterials.[31,32] We also estimated that the SiQD particle size is around 5 nm using the 518.8 cm^{-1} Raman peak based on the theoretical calculation,[31] which is in agreement with our TEM observation (Figure 1d).

Fourier transform infrared spectroscopy (FTIR) and X-ray photoelectron spectroscopy (XPS) were further used to identify the surface functionalities of the SiQDs. Figure 2a shows emphatic bands including the stretching vibration of Si−OR/Si−O−Si between 1000 and 1200 cm^{-1}[16] and vibrational scissoring and symmetric bending of $Si-CH_2$ at 1352 cm^{-1}.[19] Moreover, the peak at 2935 cm^{-1} is attributed to stretching vibrations of methyl groups, while the peaks at 3230 and 3367 cm^{-1} are attributed to the symmetric and stretching vibration of O−H, respectively.[20] On the other hand, the XPS result shows five major peaks attributed to Si 2p (102.2 eV), Si 2s (153.3 eV), C 1s (284.4 eV), N 1s (398.8 eV), and O 1s

https://doi.org/10.1021/acsomega.1c04467
ACS Omega 2022, 7, 223−229

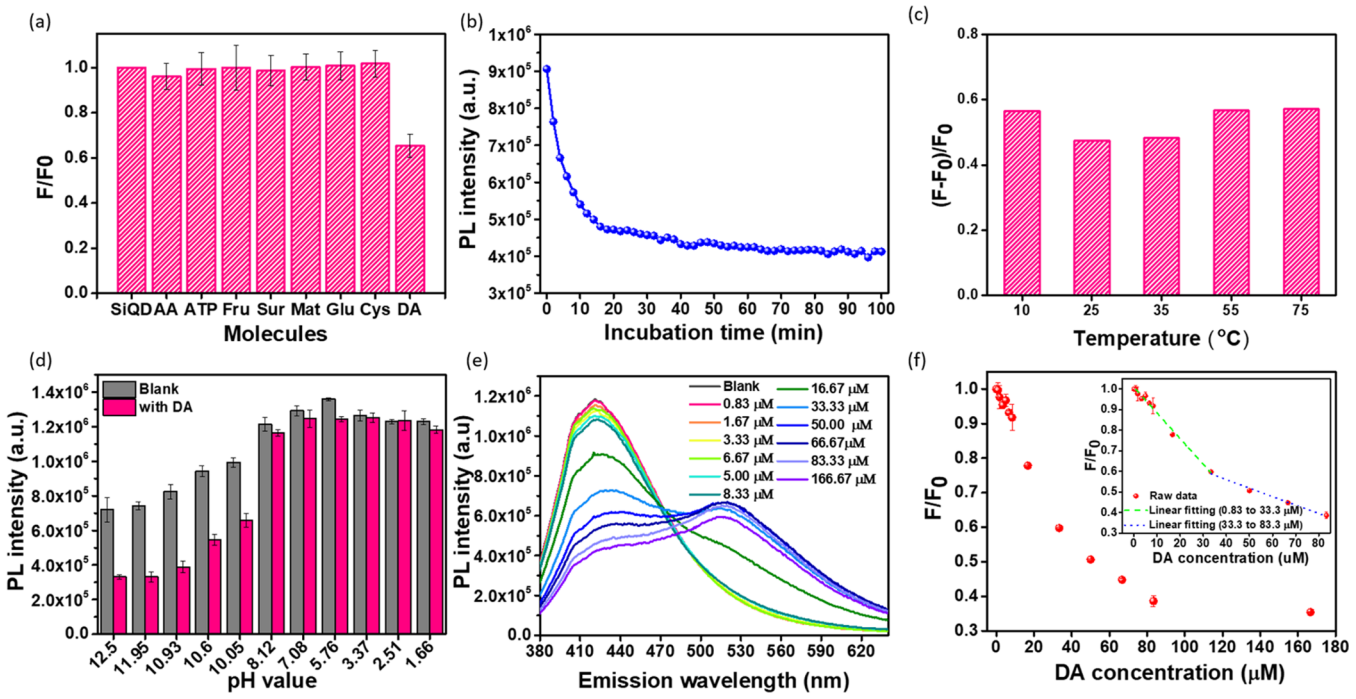

Figure 3. Dopamine detection with SiQDs. (a) Selectivity of SiQDs with different molecules (all of the concentrations were 83.3 μM in pH 10.05 at 25 °C). (b) PL Stability of SiQDs with different incubation times (under 83.3 μM DA in pH 10.93 at 25 °C). The PL quenching of SiQDs with the addition of 83.3 μM DA at different (c) temperatures (in pH 10.60) and (d) pH values (at 25 °C). (e) PL spectra of SiQDs with DA at different concentrations (after 1 h incubation in pH 10.93 at 25 °C). (f) Plot of the DA concentration versus PL intensity ratio of F/F_0 of SiQDs.

(531.9 eV) (Figure 2b),[33] indicating the composition of SiQDs. Figure 2c–f additionally shows high-resolution XPS spectra to study the chemical bonds. The C 1s spectrum suggests several chemical bonds including Si–C of SiC_x (x < 1) (282.9 eV), Si–C of SiC (283.5 eV),[19,34] C–C/C═C (284.3 eV), C–N (285.2 eV), C–OH/C–O–C (286.3 eV), and C═O (287.7 eV) (Figure 2c),[19] while the O 1s spectrum demonstrates three peaks assigned to Si–O (530.3 eV),[19] C–O (532.4 eV),[33] and Si–OH (534.8 eV)[35] (Figure 2d). Moreover, the N 1s spectrum indicates several bonds including Si–N (397.7 eV), C–N (398.3 eV), C–NH_2(399.6 eV), and NH_2(401.3 eV) (Figure 2e),[19] and the Si 2p spectrum demonstrates three Si-related bonds including Si–C (100.2 eV), Si–N (101.2 eV), and Si–O (102.3 eV) (Figure 2f).[19] Based on the abovementioned results, it is evident that monodispersed nanometer-sized SiQDs with stable PL emission and abundant surface functionalities can be synthesized in one step under ambient conditions using microplasmas.

To evaluate the selectivity of the label-free biomolecular detection with plasma-synthesized SiQDs, the PL responses of SiQDs with selected common biomolecules including dopamine (DA), ascorbic acid (AA), adenosine triphosphate (ATP), fructose (Fru), sucrose (Sur), maltose (Mat), glutamic acid (Glu), and cysteine (Cys) at 83.3 μM concentration were studied. The experimental details can be found in the Supporting Information. The PL intensities of SiQDs with different molecules were collected using PL spectroscopy, and the selectivity result is shown in Figure 3a, where F_0 and F are the PL intensities of SiQDs in the absence and the presence of the biomarkers, respectively. The ratio of F to F_0 (F/F_0) was additionally calculated to estimate the PL quenching of SiQDs with different analytes and used as an index of selectivity. It is found that SiQDs show similar PL intensities with the addition of most biomarkers except for DA. Interestingly, a significant decrease in the PL intensity of SiQDs with DA was observed, indicated by the low F/F_0 (Figure 3a). This result suggests that SiQDs can be used as a PL probe to detect the existence of DA in solution. We further studied the effects of incubation time, temperature, and pH values on DA detection using SiQDs. Figure 3b shows that the PL intensity of SiQDs decreased rapidly in the first 10 min, and then reduced slowly from 10 to 60 min. After 60 min, the PL intensity of SiQDs was stable. This observation suggests that the SiQDs can be used to detect DA in a short time. Moreover, the SiQDs exhibit similar PL responses under different temperatures from 10 to 75 °C (Figure 3c), suggesting that the SiQDs can be used for both *in vivo* and *in vitro* DA detection. Furthermore, it is noted that the PL intensities of the SiQDs were similar from pH 1.66 to 8.12, while the large fluorescence quenching occurred gradually with pH ranging from 8.12 to 12.5, indicating that DA detection with SiQDs is sensitive in basic conditions (Figure 3d). Figure 3e shows the PL spectra of SiQDs in different concentrations of DA. It is found that the PL intensities of SiQDs at emission at 420 nm decreased gradually with the increased DA concentrations. We further analyzed the detection quantitatively, and Figure 3f shows the result of F/F_0 estimated from Figure 3e as a function of the DA concentration. Based on the result, dual linear relationships between F/F_0 and the DA concentration can be established, including $F/F_0 = -0.0121C + 1.00$ for 0.83 to 33.33 μM of the DA concentration and $F/F_0 = -0.0049C + 0.76$ for 33.3 to 83.3 μM of the DA concentration ($R^2 > 0.99$ for both cases, and C denotes the DA concentration), as shown in the inset of Figure 3f. Moreover, the detection limit of DA is estimated to be 0.32 μM with the $3\sigma/S$ rule, where σ and S denote the standard deviations for the blank solution ($n = 15$) and the slope of the correlation line, respectively.

https://doi.org/10.1021/acsomega.1c04467
ACS Omega 2022, 7, 223–229

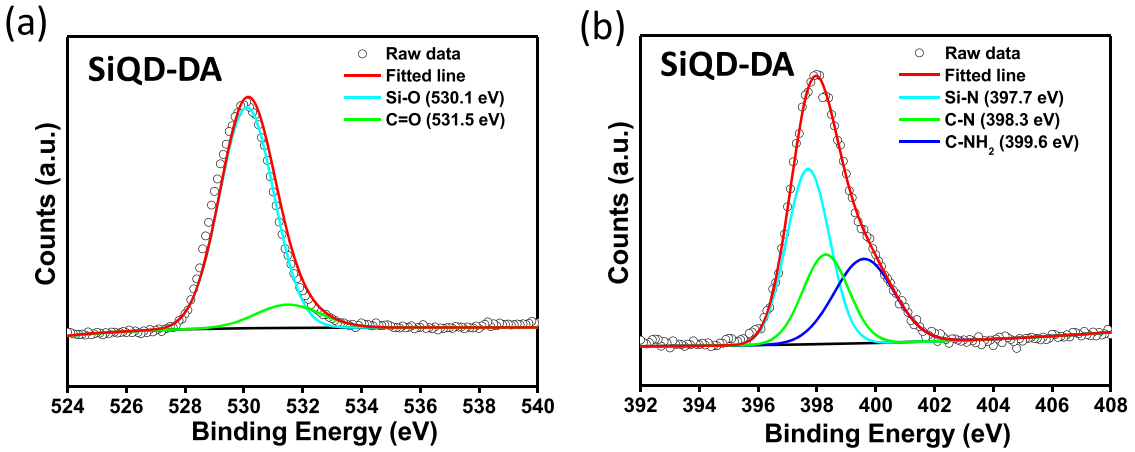

Figure 4. XPS spectra of SiQD and SiQD-DA. (a) O 1s XPS spectrum of SiQD-DA. (b) N 1s XPS spectrum of SiQD-DA.

We additionally tested the response of the synthesized SiQDs toward other biomolecules containing an alkyl amine group, consisting of epinephrine (EP), tyramine, and phenethylamine (Figure S1). Interestingly, the PL intensity of SiQDs is only affected upon the addition of EP after 1 h of mixing both in neutral (pH 7.09) and alkaline (pH 10.90) conditions at 25 °C. No PL intensity changes are observed in the case of tyramine and phenethylamine. It is also noted that EP exhibits a higher response in pH 7.09 than that in pH 10.90, while DA shows a high response in alkaline conditions (Figure 3d), implying that a different PL quenching mechanism might have occurred during the EP detection. Nonetheless, our work suggests a possibility to detect DA selectively by controlling the pH value during the sensing.[11]

To study the possible molecular interaction between the SiQDs and DA, we have additionally performed the XPS measurement of SiQDs and a mixture of SiQDs and DA (denote as SiQD-DA). Figure 4 shows the XPS result, and it is noticed that the XPS peaks of silanol (Si−OH) and N−H bonds on SiQD surfaces (Figure 4a,b) disappeared after adding DA. This finding suggests the occurrence of molecular interaction between silanol groups (−SiOH) and the N−H bond of SiQDs and DA via possible hydrogen bonds or electrostatic force. Previous work reports that DA can be oxidized to form dopamine−quinone (DA−Q) in alkaline solutions, which is an electron acceptor and thus can quench the PL intensities of PL materials.[14] Moreover, the hydrogen bonds can be generated between the silanol groups (−SiOH) of Si-based nanomaterials and DA−Q.[14] To further understand the energy transfer between SiQDs and DA−Q, UV−vis absorbance spectroscopy and PL spectroscopy were performed. Figure S2 shows the PL spectrum of SiQDs and the UV−vis absorbance spectrum of DA−Q. Clearly, an overlap between the PL spectrum of SiQDs and the absorption spectrum of DA−Q is observed, suggesting that the fluorescence resonance energy transfer (FRET) between SiQDs and DA could have occurred and further induced the PL quenching of SiQDs during the DA sensing.[7] Our result is in agreement with previous work.[7] Overall, it is envisaged that the fluorescence energy from the photoexcited SiQDs (i.e., energy donor) can be transferred to the DA−Q (i.e., energy acceptor) attracted onto the SiQD surfaces in alkaline conditions to complete the PL quenching process. The surface functionality-induced conjugation of SiQDs and DA−Q can shorten the distance between each other and further enhance the FRET for more sensitive DA detection,[7] leading to label-free detection of DA using plasma-synthesized SiQDs with high sensitivity and selectivity.

The UV−vis absorption of EP, tyramine, and phenethylamine was further measured at neutral and alkaline conditions (Figure S3b−d) to clarify the sensitivity of SiQDs toward alkyl amine-containing biomolecules. As has been revealed in Figure S2, the introduction of DA at alkaline conditions can result in a FRET quenching mechanism. Meanwhile, EP exhibits quite a strong absorption around 270−370 nm (Figure S3b), overlapping with the 340 nm excitation wavelength of SiQDs, which can lead to PL quenching due to the inner filter effect (IFE).[11] The absorptions of tyramine (Figure S3c) and phenethylamine (Figure S3d), on the other hand, are below 330 nm and thus will not exhibit any FRET or IFE responsible for the PL quenching. Therefore, it can be concluded that in addition to the needs of molecular interactions, a FRET or IFE phenomenon is also critical to induce PL quenching.

3. CONCLUSIONS

In summary, we have reported a simple and scalable method to synthesize surface-functionalized SiQDs with defined structures at ambient conditions using microplasmas and demonstrated that the plasma-synthesized SiQDs can be used directly for quantitative label-free detection of DA without any special treatments. The plasma-synthesized SiQDs show stable colloidal dispersion with long-term stability and stable room-temperature blue photoluminescence emission at 420 nm. Importantly, the abundant surface functionalities on the SiQD surfaces can selectively attract the DA molecules onto the SiQD surfaces via a hydrogen bond without any complex surface modifications. The unique synergistic effect due to the surface functionality-induced molecular interaction and FRET-induced PL quenching between DA and SiQDs leads to the superior sensing of DA, with a wide sensing range from 0.83 to 83.33 μM and a low detection limit of 0.32 μM. Our work opens a new direction for scalable synthesis of colloidal nanomaterials for emerging applications including nanosensing, nanocatalysis, optoelectronics, and biomedical applications such as bioimaging and drug delivery.

4. EXPERIMENTAL SECTION

4.1. Synthesis of SiQDs. SiQDs were synthesized in aqueous solutions using a direct current (dc) microplasma

https://doi.org/10.1021/acsomega.1c04467
ACS Omega 2022, 7, 223−229

electrochemical reactor operated at ambient conditions, shown in Figure 1a. The precursor solution was prepared by mixing AEAPTMS (0.2 mL), 0.1 M NaOH(2.5 mL), and DI water (9.8 mL). The experimental setup is similar to our previous studies.[23,24] In brief, a flow of 25 sccm argon (Ar) was introduced in a hollow stainless steel capillary (i.d. = 180 μm) to facilitate the formation of a microplasma. The process was kept at a 7 mA plasma current and 0.5 h reaction time. Details of materials and chemicals used in this work and plasma synthesis can be found in the Supporting Information.

4.2. Characterization. Absorbance spectroscopy was carried out using a JASCO V676 absorbance spectrophotometer. PL spectroscopy was performed using a commercial spectrometer (Horiba JobinYvon Nanolog-3 spectrofluorometer). Micro-Raman measurement was conducted using a JASCO 5100 spectrometer (laser excitation wavelength λ = 532. nm). A silicon wafer was used to calibrate Raman shifts using the 520 cm^{-1} peak. FITR spectra were collected using an FTIR-iS10 equipped with an attenuated total reflection (ATR) module. TEM was performed using a cold-field emission TEM (FEI Tecnai G2 F-20 S-TWIN) with an accelerating voltage of 200 kV. XPS (ULVAC-PHI, PHI Quantera SXM, Japan) was carried out using a monochromatic Al Kα X-ray radiation (10 kV, 10 mA). Details of characterization can be found in the Supporting Information.

4.3. DA Detection. DA solutions with different concentrations (2.5 mL) were mixed with the SiQD solution (0.33 mg/mL, 0.5 mL). After 1 h of incubation time, the PL intensity of the mixed dispersion was measured at a 340 nm excitation wavelength. To study the selective detection, each solution including dopamine (DA), ascorbic acid (AA), adenosine triphosphate (ATP), D-fructose (Fru), sucrose (Sur), maltose (Mat), glutamic acid (Glu), cysteine (Cys), epinephrine (EP), tyramine, and phenethylamine (2.5 mL, 100 μM) were mixed with SiQD solutions. After 1 h of incubation time, the PL intensity of the mixed dispersion was measured at a 340 nm excitation wavelength. To study the pH effect, 1 M phosphate-buffered saline (PBS) solutions with different pH values were prepared by adjusting the pH values with HCl and NaOH. Then, DA solutions with different concentrations (2.2 mL) were mixed with the SiQD solution (0.5 mL) and pH-adjusted PBS solutions (0.3 mL). After 1 h of incubation time, the PL intensity of the mixed dispersion was measured at a 340 nm excitation wavelength. The details of the sensing study can be found in the Supporting Information.

■ ASSOCIATED CONTENT

Supporting Information

The Supporting Information is available free of charge at https://pubs.acs.org/doi/10.1021/acsomega.1c04467.

Supporting Information including material synthesis and characterizations and additional analysis including UV−vis absorption and PL measurements (PDF)

■ AUTHOR INFORMATION

Corresponding Author

Wei-Hung Chiang − *Department of Chemical Engineering, National Taiwan University of Science and Technology, Taipei 10607, Taiwan;* orcid.org/0000-0002-6350-6696; Email: whchiang@mail.ntust.edu.tw

Authors

Gui-Yi Chang − *Department of Chemical Engineering, National Taiwan University of Science and Technology, Taipei 10607, Taiwan*

Darwin Kurniawan − *Department of Chemical Engineering, National Taiwan University of Science and Technology, Taipei 10607, Taiwan;* orcid.org/0000-0003-4198-7641

Yi-Ju Chang − *Department of Chemical Engineering, National Taiwan University of Science and Technology, Taipei 10607, Taiwan*

Complete contact information is available at: https://pubs.acs.org/10.1021/acsomega.1c04467

Author Contributions

All authors have given approval to the final version of the manuscript.

Notes

The authors declare no competing financial interest.

■ ACKNOWLEDGMENTS

This work was supported by the Ministry of Science and Technology of Taiwan (MOST grant nos. 109-2923-E-011-003-MY3, 110-NU-E-011-00-NU, and 110-2628-E-011-003).

■ REFERENCES

(1) Robinson, D. L.; Hermans, A.; Seipel, A. T.; Wightman, R. M. Monitoring Rapid Chemical Communication in the Brain. *Chem. Rev.* **2008**, *108*, 2554−2584.

(2) Wu, D.; Xie, H.; Lu, H.; Li, W.; Zhang, Q. Sensitive determination of norepinephrine, epinephrine, dopamine and 5-hydroxytryptamine by coupling HPLC with [Ag(HIO6)2](5-)-luminol chemiluminescence detection. *Biomed. Chromatogr.* **2016**, *30*, 1458−66.

(3) Zen, J.-M.; Chen, P.-J. A Selective Voltammetric Method for Uric Acid and Dopamine Detection Using Clay-Modified Electrodes. *Anal. Chem.* **1997**, *69*, 5087−5093.

(4) Zhang, K.; Liu, Y.; Wang, Y.; Zhang, R.; Liu, J.; Wei, J.; Qian, H.; Qian, K.; Chen, R.; Liu, B. Quantitative SERS Detection of Dopamine in Cerebrospinal Fluid by Dual-Recognition-Induced Hot Spot Generation. *ACS Appl. Mater. Interfaces* **2018**, *10*, 15388−15394.

(5) Phung, V. D.; Jung, W. S.; Nguyen, T. A.; Kim, J. H.; Lee, S. W. Reliable and Quantitative SERS Detection of Dopamine Levels in Human Blood Plasma Using a Plasmonic Au/Ag Nanocluster Substrate. *Nanoscale* **2018**, *10*, 22493−22503.

(6) Badillo-Ramírez, I.; Saniger, J. M.; Popp, J.; Cialla-May, D. SERS Characterization of Dopamine and In Situ Dopamine Polymerization on Silver Nanoparticles. *Phys. Chem. Chem. Phys.* **2021**, *23*, 12158−12170.

(7) Zhang, X.; Chen, X.; Kai, S.; Wang, H.-Y.; Yang, J.; Wu, F.-G.; Chen, Z. Highly sensitive and selective detection of dopamine using one-pot synthesized highly photoluminescent silicon nanoparticles. *Anal. Chem.* **2015**, *87*, 3360−5.

(8) Kumar, A.; Asu, S.; Mukherjee, P.; Singh, P.; Kumari, A.; Sahu, S. K. Single-Step Synthesis of N-Doped Carbon Dots and Applied for Dopamine Sensing, In Vitro Multicolor Cellular Imaging as well as Fluorescent Ink. *J. Photochem. Photobiol. A* **2021**, *406*, No. 113019.

(9) Ma, Y.; Chen, A. Y.; Xie, X. F.; Wang, X. Y.; Wang, D.; Wang, P.; Li, H. J.; Yang, J. H.; Li, Y. Doping Effect and Fluorescence Quenching Mechanism of N-Doped Graphene Quantum Dots in the Detection of Dopamine. *Talanta* **2019**, *196*, 563−571.

(10) Mu, Q.; Xu, H.; Li, Y.; Ma, S.; Zhong, X. Adenosine capped QDs based fluorescent sensor for detection of dopamine with high selectivity and sensitivity. *Analyst* **2014**, *139*, 93−8.

(11) Kurniawan, D.; Jhang, R.-C.; Ostrikov, K. K.; Chiang, W.-H. Microplasma-Tunable Graphene Quantum Dots for Ultrasensitive

and Selective Detection of Cancer and Neurotransmitter Biomarkers. *ACS Appl. Mater. Interfaces* **2021**, *13*, 34572−34583.
(12) Gonzalez, C. M.; Veinot, J. G. C. Silicon nanocrystals for the development of sensing platforms. *J. Mater. Chem. C* **2016**, *4*, 4836−4846.
(13) He, Y.; Fan, C.; Lee, S.-T. Silicon nanostructures for bioapplications. *Nano Today* **2010**, *5*, 282−295.
(14) Xiangzhao, A.; Qiang, M.; Xingguang, S. Nanosensor for Dopamine and Glutathione based on the Quenching and Recovery of the Fluorescence of Silica-Coated Quantum Dots. *Microchim. Acta* **2013**, *180*, 269−277.
(15) Atkins, T. M.; Thibert, A.; Larsen, D. S.; Dey, S.; Browning, N. D.; Kauzlarich, S. M. Femtosecond ligand/core dynamics of microwave-assisted synthesized silicon quantum dots in aqueous solution. *J. Am. Chem. Soc.* **2011**, *133*, 20664−20667.
(16) Gong, T.; Li, Y.; Lei, B.; Zhang, X.; Liu, Y.; Zhang, H. Solid-state silicon nanoparticles with color-tunable photoluminescence and multifunctional applications. *J. Mater. Chem. C* **2019**, *7*, 5962−5969.
(17) He, Y.; Zhong, Y.; Peng, F.; Wei, X.; Su, Y.; Lu, Y.; Su, S.; Gu, W.; Liao, L.; Lee, S. T. One-pot microwave synthesis of water-dispersible, ultraphoto- and pH-stable, and highly fluorescent silicon quantum dots. *J. Am. Chem. Soc.* **2011**, *133*, 14192−14195.
(18) Wei, N.; Wei, M.-X.; Huang, B.-H.; Guo, X.-F.; Wang, H. One-pot facile synthesis of green-emitting fluorescent silicon quantum dots for the highly selective and sensitive detection of nitrite in food samples. *Dyes Pigm.* **2021**, *184*, No. 108848.
(19) Wu, J.; Dai, J.; Shao, Y.; Sun, Y. One-step synthesis of fluorescent silicon quantum dots (Si-QDs) and their application for cell imaging. *RSC Adv.* **2015**, *5*, 83581−83587.
(20) Zhang, Z.; Wei, C.; Ma, W.; Li, J.; Xiao, X.; Zhao, D. One-Step Hydrothermal Synthesis of Yellow and Green Emitting Silicon Quantum Dots with Synergistic Effect. *Nanomaterials* **2019**, *9*, No. 466.
(21) Mariotti, D.; Sankaran, R. M. Microplasmas for nanomaterials synthesis. *J. Phys. D: Appl. Phys.* **2010**, *43*, No. 323001.
(22) Chiang, W.-H.; Mariotti, D.; Sankaran, R. M.; Eden, J. G.; Ostrikov, K. K. Microplasmas for Advanced Materials and Devices. *Adv. Mater.* **2020**, *32*, No. 1905508.
(23) Yeh, P.-C.; Yoon, S.; Kurniawan, D.; Chung, Y. G.; Chiang, W.-H. Unraveling the Fluorescence Quenching of Colloidal Graphene Quantum Dots for Selective Metal Ion Detection. *ACS Appl. Nano Mater.* **2021**, *4*, 5636−5642.
(24) Kurniawan, D.; Chiang, W. H. Microplasma-enabled colloidal nitrogen-doped graphene quantum dots for broad-range fluorescent pH sensors. *Carbon* **2020**, *167*, 675−684.
(25) Zhu, M. J.; Lerum, M. Z.; Chen, W. How To Prepare Reproducible, Homogeneous, and Hydrolytically Stable Aminosilane-Derived Layers on Silica. *Langmuir* **2012**, *28*, 416−423.
(26) Wang, J.; Liu, Y.; Peng, F.; Chen, C.; He, Y.; Ma, H.; Cao, L.; Sun, S. A General Route to Efficient Functionalization of Silicon Quantum Dots for High-Performance Fluorescent Probes. *Small* **2012**, *8*, 2430−2435.
(27) Zhao, D.; Song, H.; Hao, L.; Liu, X.; Zhang, L.; Lv, Y. Luminescent ZnO quantum dots for sensitive and selective detection of dopamine. *Talanta* **2013**, *107*, 133−139.
(28) Li, D.; Xu, X.; Zhou, P.; Huang, Y.; Feng, Y.; Gu, Y.; Wang, M.; Liu, Y. A facile synthesis of hybrid silicon quantum dots and fluorescent detection of bovine hemoglobin. *New J. Chem.* **2019**, *43*, 19338−19343.
(29) Bagabas, A. A.; Gondal, M. A.; Dastageer, M. A.; Al-Muhanna, A. A.; Alanazi, T. H.; Ababtain, M. A. A study of laser-induced blue emission with nanosecond decay of silicon nanoparticles synthesized by a chemical etching method. *Nanotechnology* **2009**, *20*, No. 355703.
(30) Zhang, Y.; Han, X.; Zhang, J.; Liu, Y.; Huang, H.; Ming, H.; Lee, S. T.; Kang, Z. Photoluminescence of silicon quantum dots in nanospheres. *Nanoscale* **2012**, *4*, 7760−7765.
(31) Cheng, W.; Ren, S.-F. Calculations on the size effects of Raman intensities of silicon quantum dots. *Phys. Rev. B* **2002**, *65*, No. 205305.
(32) Faraci, G.; Gibilisco, S.; Pennisi, A. R.; Faraci, C. Quantum size effects in Raman spectra of Si nanocrystals. *J. Appl. Phys.* **2011**, *109*, No. 074311.
(33) Luo, L.; Song, Y.; Zhu, C.; Fu, S.; Shi, Q.; Sun, Y.-M.; Jia, B.; Du, D.; Xu, Z.-L.; Lin, Y. Fluorescent silicon nanoparticles-based ratiometric fluorescence immunoassay for sensitive detection of ethyl carbamate in red wine. *Sens. Actuators B Chem.* **2018**, *255*, 2742−2749.
(34) Wen, G.; Zeng, X.; Wen, X.; Liao, W. Photoluminescence properties and crystallization of silicon quantum dots in hydrogenated amorphous Si-rich silicon carbide films. *J. Appl. Phys.* **2014**, *115*, No. 164303.
(35) Soulé, S.; Allouche, J.; Dupin, J.-C.; Courreges, C.; Plantier, F.; Ojo, W.-S.; Coppel, Y.; Nayral, C.; Delpech, F.; Martinez, H. Thermoresponsive gold nanoshell@mesoporous silica nano-assemblies: an XPS/NMR survey. *Phys. Chem. Chem. Phys.* **2015**, *17*, 28719−28728.

https://doi.org/10.1021/acsomega.1c04467
ACS Omega 2022, 7, 223−229